The Pyroptosis-Related Signature Predicts Prognosis and Indicates New Treatment Targets in Pancreatic Cancer

Zhenyu Zhao
Jinan University
Hai Yan
Flushing Hospital Medical Center
Xiao Li
Shanxi Province Cancer Hospital, Chinese Academy of Medical Sciences, Cancer Hospital Affiliated to Shanxi Medical University
Yanling Yu
Shanxi Province Cancer Hospital, Chinese Academy of Medical Sciences, Cancer Hospital Affiliated to Shanxi Medical University
Chunyan Wang (chunyanwang2007@163.com)
Shanxi Province Cancer Hospital, Chinese Academy of Medical Sciences, Cancer Hospital Affiliated to Shanxi Medical University

Research Article

Keywords: Pyroptosis, PAAD, PRG, TME, PFS

Posted Date: May 13th, 2022

DOI: https://doi.org/10.21203/rs.3.rs-1636634/v1

Abstract

Purpose

Pancreatic adenocarcinoma (PAAD) is a malignant tumor leading cause of cancer death worldwide. Pyroptosis is a recently identified inflammatory cell death that is associated with tumor progression, prognosis, and treatment response. Our study investigated the potential roles of pyroptosis-related genes (PRGs) in the tumor microenvironment (TME).

Methods

We explored 48 PRGs in 350 PAAD samples from genetic and transcriptional fields. Immunocyte subsets in three subgroups were investigated and we found that B-PRGcluster was correlated with PAAD progression and TME cell- infiltrating characteristics. Then, we established a highly accurate nomogram for improving the clinical applicability of the PRG_score. Moreover, we evaluated chemotherapeutic agents used for PAAD to assess the susceptibility of patients in low-risk and high-risk groups to these agents.

Results

Significant differences in the genetic landscape and expression levels of PRGs between PAAD and normal samples indicated a potential role for PRGs in the development of PAAD. The prognosis of PAAD patient was significantly correlated with the expression levels of PRG. The infiltration immune cells in B_PRGcluster was identified which play the role of PRG in the TME of PAAD. The PFS of 1,2 and 3 years had higher accuracy, and TP53 was the second most frequently mutated gene after KARS in high-risk and low-risk groups classified by PRG-score. The rise of Risk Score indicated that the number of patients in Dead state was significantly increased, and the gene expression showed a positive correlation with Risk Score. The correlation between Tumor Burden Mutation and risk score showed a significant positive correlation.

Conclusion

Our investigation of PRGs in PAAD revealed their potential roles in the TME, clinicopathological features, and prognosis. These findings highlight a new insight in the understanding of PRGs in PAAD and offer a novel approach to immunotherapy strategies.

Introduction

Pancreatic adenocarcinoma (PAAD), as a common gastrointestinal tumor, is lethal and aggressive with a 5-year survival rate of only 2–9%, making it the seventh leading cause of cancer deaths in both sexes and

accounting for 4.5% of the global cancer deaths in 2018. It is expected to overtake colorectal and breast cancer as the second leading cause of cancer-related deaths after lung cancer by 2030 (Rahib, Smith et al. 2014). Even though great advances have been made in traditional therapies for PAAD, including surgery, chemotherapy, and radiotherapy, the prognosis of patients with PAAD remains poor, mainly due to distant metastasis of brain and local invasion (Rhim, Mirek et al. 2012, Nielsen, Quaranta et al. 2016, Ji, Ma et al. 2021). Other treatment strategies, such as combination chemotherapy, molecular-targeted therapy, and immune checkpoint inhibitors, have limited efficacy due to the inherent chemotherapy and immune resistance (den Butter, van Bockel et al. 1988, Iacobuzio-Donahue, Fu et al. 2009, Pipas, Zaki et al. 2012, Huang, Zhang et al. 2021). PAAD remains asymptomatic in the early stages and the appearance of jaundice was usually accompanied by the diagnosis of locally advanced unresectable tumors. Less than 20% of patients meet the criteria for surgical resection (Konstantinidis, Warshaw et al. 2013, Wang, Zhang et al. 2022).

Pyroptosis is a new inflammatory programmed cell death (PCD) discovered after apoptosis and cell necrosis(Cookson and Brennan 2001). Cytopyrosis and apoptosis have some similar characteristics. The cells with Pyroptosis also present with nuclear shrinkage, DNA fragmentation and positive Annexin staining, etc. The dead cells also resemble necrotic cells that both cells are swollen then burst and cellular contents were released, causing an inflammatory response (Yang, Daniel et al. 1989, Bergsbaken, Fink et al. 2009). The necrotic cells are characterized by the activation of inflammatory cysteine proteases (caspases-1, 4, 5, and 11) in inflammasomes and the secretion of pro-inflammatory cytokines interleukin-1β and interleukin-18(Bregetzer 1989). In an unregulated pathway, CASP4, 5, and 11 can be activated by bacterial lipopolysaccharide (LPS) and then cleaved directly into GSDMD to induce cellular purulence (Shi, Zhao et al. 2015). It can be seen that cellular apoptosis is regulated by multiple genes and produces pro-inflammatory effects while causing cellular lysis (Bai, Xu et al. 2022). Cellular apoptosis, as a new inflammatory programmed cell death, is widely involved in the occurrence and development of various diseases.

Materials And Methods

Data sources

Gene expression profiles of pancreatic cancer have been obtained from Gene Expression Omnibus (GEO) (https://www.ncbi.nlm.nih.gov/geo/) and the Cancer Genome Atlas (TCGA) (https://portal.gdc.cancer.gov/), and patient-specific clinical information is essential. The RNAseq data in the level 3 HTSeq-FPKM format in the TCGA (https://portal.gdc.cancer.gov/) PAAD project has been converted from the FPKM (Fregments Per Kilobase per Million) format to the TPM (transcripts per million reads) format(Conesa, Madrigal et al. 2016). Several datasets downloaded from the GEO database have been combined and batch effects eliminated rigorously using the “Combat” algorithm. We have downloaded clinical variables, including T stage, N stage, risk score and survival status from 158 patients with TCGA.

Consensus clustering analysis of PRGs

Pyroptosis-related genes have been downloaded from the MSigDB database, and some have been added to the already reported literature(Ye, Dai et al. 2021). The R-package "ConsensusClusterPlus" was used for consistent unsupervised clustering analysis, which categorised patients into different molecular subtypes based on PRG expression. The clustering was performed according to the following criteria: First, the cumulative distribution function (CDF) curve gradually and smoothly increased. Second, no group has a small sample size. Finally, after clustering, the correlation within groups increased and the correlation between groups decreased. To investigate differences in PRGs during biological processes, a gene set mutation analysis (GSVA) was performed on the hallmark gene set (c2). Cp.kegg.v7.2) from MSigDB database.

Relationship between molecular subtypes with the clinical features and prognosis of PAAD

The clinical value of the two subtypes identified by consensus clustering has been tested by comparing the relationship between molecular subtypes, clinical pathology features and prognosis. Patient characteristics include T stage, N stage, risk score and survival status. In addition, Kaplan-Meier curves generated by R package "surviving" and "survivors" were used to assess differences in RFS between subtypes.

Correlations of molecular subtypes with TME in PAAD

We evaluated the immune and stromal scores of each patient using the ESTIMATE algorithm. In addition, a score of 22 human immune cell subsets per PAAD sample was calculated using the CIBERSORT algorithm(Newman, Liu et al. 2015). In addition, the level of immunocyte infiltration of TME in PAAD was determined using a single sample gene set enrichment analysis (ssGSEA) algorithm(Rooney, Shukla et al. 2015).

DEG identification and functional annotation

Differentially expressed genes between the different pyroptosis subtypes were identified applying the' limma' package in R, with the absolute value of fold change set to greater than 1.5 and adjusted p value < 0.05. In order to further explore the potential functions of differentially expressed genes related to pyroptosis pattern and identify the functions and enrichment pathways of related genes, the "clustering analysis" R package was utilized for functional enrichment analysis of differential genes.

Construction of the pyroptosis-related prognostic PRG_score

PRG_score has been calculated to quantify the pattern of pyroptosis in a single tumor. First, we have identified DEG that was relevant to PAAD RFS by univariate Cox regression analysis of DEG. Second, the patients were divided into different subtype groups (pyroptosis gene subtype A, pyroptosis gene subtype B and pyroptosis gene subtype C). On the basis of prognostic PRGs expression, an unsupervised clustering method was used for in-depth analysis. Finally, all PAAD patients were randomly divided into

training and test groups at a ratio of 1:1, and then adopted the former to construct a prognostic PRG_score associated with pyroptosis. In short, based on the prognostic genes associated with pyroptosis, the Lasso Cox regression algorithm was used to minimize the risk of over-fitting using "GLMN", and the R-package was used to analyze the trajectories of numerous variables, using 10-fold cross-validation to establish the model. Candidate genes were selected using multivariate Cox analysis to establish prognostic PRG_score in the training set.

The PRG_score was calculated as follows: PRG _ score = σ (Expi * Coefi), whereas coefi and expi represent the risk factor of each PRG gene and its corresponding expression level. All the patients in the training set were divided into three groups, and the survival curves were drawn according to the groups. The R package "ggpolt2" has then been utilized for principal component analysis (PCA). Similarly, the testing and all groups were divided into low-risk and high-risk groups, and each group was subjected to Kaplan-Meier survival analysis and generated receiver operating characteristics (ROC) curves.

Clinical correlation and stratification analyses of the prognostic PRG_score

The relationship between PRG_score and clinical features was investigated using Chi-square test. To assess whether the risk score was independent of other available clinical pathology features, the univariate and multivariate analyse were performed on the training and test sets. In addition, stratified analysis was performed to determine whether PRG_score retained its predictive power in different subgroups based on clinical features.

To appraise the proportion of TIICs in the TME, the abundance of 22 infiltrating immune cells in heterogeneous samples from the low-risk and high-risk groups was quantified applying CIBERSORT. We explored the association of 22 components of infiltrating immune cells with 7 genes in PRG_score. We also depicted boxplot to examine the differential expression of immune checkpoints between the low-and high-scoring groups. In addition, we analyzed the relationship between these two risk groups and MSI and CSC.

Mutation and drug susceptibility analysis

To identify somatic mutations in PAAD patients between the high-risk and low-risk groups, a mutation annotation format (MAF) for the TCGA database was generated using the "MAF Tools" R package. We also calculated the tumor mutation burden (TMB) score for each patient with PAAD in both groups. With the purpose to quest the difference of chemotherapeutic effects between the two groups, the "pRRophetic" software package was used to calculate the semi-inhibitory concentration (IC50) values of commonly used chemotherapeutic drugs for the treatment of PAAD.

Establishment and validation of a nomogram scoring system

Based on the results of the independent prognostic analysis, predictive nomograms were developed using the "RMS" package, with clinical features and risk scores. In the Nomogram scoring system, each variable was matched with a score, and the total score was obtained by adding the scores of all the variables in

each sample(Iasonos, Schrag et al. 2008). The Nomogram was evaluated using a time-dependent ROC curve for 3-,5-, and 10-year survival. Calibration plots of the nomogram were used to describe the predicted values between the predicted 3-,5-, and 10-year survival events and the actually observed results.

Statistical analysis

All statistical analyses were performed using R version 4.1.0. The difference was statistically significant ($p < .05$).

Results

Differential expression of PRG in transcription level of PAAD samples

We have made a rigorous differential analysis of the expression of 46 PRGs in pancreatic cancer. Containing 350 samples, and the results indicated that there were 46 PRGs with significant differences in transcription level between tumor and normal tissues. Moreover, more interestingly, compared with normal tissues, the transcription level of all PRGs is much higher in tumor tissues. In general, mRNA level of a gene is affected by a variety of environmental variables, such as DNA methylation and transcription factors, and mRNA stability is also a major factor. Gene such as GSDMC are molecules of that Gasdermin family, which is Pore-forming proteins that cause membrane permeabilization and pyroptosis (Ding, Wang et al. 2016). Significant differences in the genetic landscape and expression levels of PRGs between PAAD and normal samples indicated a potential role for PRGs in the development of PAAD.

Identification of pyroptosis subtypes in PAAD

PRG interactions, regulatory ligation, and their prognostic value in patients with pancreatic cancer are demonstrated in a Pyroptosis network. In order to further explore the expression characteristics of PRGs in PAAD, the consensus clustering algorithm had been established on the expression profiles of the 46 PRGs. Our results show that k = 3 appears to be the best choice for categorizing the entire cohort into three subtypes (Figure 2A). Principal component analysis revealed significant differences in sample profiles for the three subtypes, with subsequent analyses showing significant statistical significance (Figure 2B). The Kaplan-Meier curve showed that the OS of patients with subtype B and C was shorter than that of patients with subtype A (log-rank test, p = 0.014; Figure 2C.Differences in clinicopathologic features and expression levels of PRGs between the three distinct subtypes was shown by heat map Figure 2d. In Figure 2D, we can see that the expression levels of most PRG in B PRGcluster are much higher than those of A and C, which indicates that the prognosis of our patient was significantly correlated with the expression levels of PRG.

Characteristics of the TME in distinct subtypes

Gene set enrichment analysis is used to assess changes in activity in the pathway/function in which the gene set is located. A comparative analysis of three different PRGcluster (A/B/C) was performed here. It

can be seen that B_PRGcluster is always enriched in the immune pathway. In contrast to A_PRGcluster, B_PRGcluster is found in the KEGG _ primary _ immune, KEGG _ CYTOKINE _ CYTOKINE _ RECEPTOR _ INTERACTION, KEGG _ INTESTINAL _ IMMUNE _ NETWORK _ FOR _ IGA _ PRODUCTION, KEGG _ TOLL _ LIKE _ RECEPTOR _ SIGNALING _ PATHWAY, KEGG _ T _ CELL _ RECEPTOR _ SIGNALING _ PATHWAY, and KEGG _ B _ CELL _ RECEPTOR _ SIGNALING _ PATHWAY. In contrast to B_PRGcluster and C_PRGcluster, the pathways through which B_PRGcluster is significantly enriched include KEGG _ NATURAL _ KILLER _ CELL _ MEDIATED _ CYTOTOXICITY, KEGG _ LEUKOCYTE _ TRAN ENDOTHYAL _ MIGRATION, KEGG _ CHEMOKINE _ SIGNAGING _ PATHWAY, KEGG_PATHWAYS_IN_CANCER.(Figure. 3A-C). For the purpose of studying the role of PRG in the TME of PAAD, we evaluated the association between the three subtypes and 22 human immunocyte subsets in each PAAD sample with the CIBERSORT algorithm. We observed a significant difference in the infection of most cells. We found that the infiltration level of most immune cells in B_PRGcluster was much higher than that of the other two PRGclusters, for example, Activated. B. cell, Activated. CD4. T. Cell, Activated. CD8. T. Cell, Immunoture. B. Cell, Eosinophil, Gamma.delta.T.cell, and so on. There were also cases in which the infiltration level of individual immune cells in B_PRGcluster was the lowest, for example, Cd56Dim. Natural. Killer. Cell (Figure. 3D).

Identification of gene subtypes based on DEGs

To explore the potential biological behavior of each of the pyroptosis patterns, 631 DEG associated with the pyroptosis subtypes were identified and analyzed for functional enrichment using the R-package "limma" (Figure 4A). These genes related to pyroptosis subtypes are significantly enriched in immune-related biological processes (Figure 4B), such as immune-related pathways as T cell activation, Leucocyte migration, Leucocyte mediated immunity, and Leucocyte cell adhesion. The KEGG analysis revealed enrichment of immune-and cancer-related pathways (Figure 4C), such as the Cytokine Cytokine Receptors Interaction, Cell adhesion molecules. All these indicate that pyroptosis plays a vital role in the tumor immune microenvironment of the patients. univariate Cox regression analysis was then performed to determine the prognostic value of a large number of subtype-related genes, and several genes related to the time of RFS were screened for subsequent analysis ($p<0.05$). To further verify this regulatory mechanism, patients were divided into two genomic subtypes based on prognostic genes by consistent clustering algorithm; Namely, gene subtype A–B. The Kaplan-Meier curve showed that patients with genotype A had the worst RFS, whereas patients with genotype B had better RFS (Figure 4F). In addition, the pyroptosis gene subtype A pattern was associated with advanced TNM stage (Figure 4E). The two pyroptosis gene subtypes showed significant differences in PRG expression, consistent with the expected results of the pyroptosis patterns（Figure 4G）.

Construction and validation of the prognostic PRG_score

PRG_score was established based on subtype-related DEG. The distribution of patients for the three PRGcluster, the two genecluster, the high-low risk, and the two Fustat types is illustrated in Figure 5A. From the observation of risk score in TCGA, we can comprehend that in the case of two subgroups of genecluster, the risk score of Gene Cluster A was much higher than that of Gene Cluster B (Figure 5B).

Additionally, A PRGcluster had the highest risk score, whereas C_PRGcluster had the lowest risk score (Figure 5C). At the same time, PRGs were grouped and compared according to the level of risk score, and we observed that the expression level of most PRGs was in direct proportion to risk score, such as CHMP2B, NOD2, HMGB1, CASP6; There were also cases where PRG expression levels were negatively correlated with risk score, such as IL6, NLRP1, GSDMA, and GZMA (Figure 5D). Next, we plotted the survival curve by grouping according to the level of risk score and found that the high-risk group had a much worse prognosis outcome (Figure E5E-G). Meanwhile, the time-dependent ROC curve was also drawn. The prediction performances at the three time points of 1 year, 3 years and 5 years were all excellent (Figure 5H-J; AUC>0.5).

Development of a nomogram to predict survival

Considering the inconvenience and clinical applicability of PRG_score in predicting the survival of patients with PAAD, a nomogram containing PRG_score and clinical pathology parameters was established to predict the incidence in 1, 2, and 3 years. Predictors included PRG score and patient stage. Our AUC experimental results on the nomogram model showed that the RFS of 1, 2, and 3 years had higher accuracy (Figure 6A) in the training set, the test set, and two external verification sets. Calibration curves also showed the accuracy of the prediction model. We judged the prediction effect of the model on the actual results by observing whether the fold lines were fitted on the diagonal (Figure 6B). Patients with PRG scores lower than the median risk score were classified as low-risk groups, while patients with PRG scores higher than the median risk score were classified as high-risk groups. The risk profile of PRG score showed that with the increase of PRG score, the survival time was decreased, and the recurrence rate was increased. We can learn that with the rise of Risk Score, the number of patients in Dead state was significantly increased, and the gene expression showed a positive correlation with Risk Score (Figure 6C-K).

Evaluation of TME and checkpoints between the high- and low-risk groups

To explore the relationship between PRG_score and the immune microenvironment, we have performed the CIBERSORT algorithm to evaluate the association between PRG_score and immune cells abundance. The results as shown in the scatter diagram exhibited that PRG_score had a negative correlation with four types of immune cells: B cells naïve, Monocytes, T cells CD8, and T cells gamma delta, and a positive correlation with Macrophages M0 and T cells regulatory (Tregs) (Figure 7A-F). At the same time, low PRG_score was accompanied by higher immune score, whereas high PRG_score was accompanied by low immune score (Figure 7G). At the same time, we also showed the correlation of several PRG with 22 immune cells in the form of heat map. As in the previous results, a positive correlation could be observed between PRG and Macrophages M0, T cells regulatory (Tregs); Moreover, a negative correlation could be observed with B cells naïve, Monocytes, T cells CD8 (Figure 7H).

Mutation and drug susceptibility analysis

We then analyzed the distribution of somatic mutations between the two PRG_score groups in the TCGA-PAAD cohort. The first ten mutated genes in the high-risk group and the low-risk group were KRAS, TP53, CDKN2A, SMAD4, TNN, RNF43, MUC16, PCDH15, RRIR1, and DAMS12 (Figure 7I-J). At the same time, the correlation between Tumor Burden Mutation and risk score was also revealed, and a significant positive correlation could be observed (Figure 7K). We next selected chemotherapeutic agents currently used for the treatment of PAAD to assess the susceptibility of patients in the low-risk and high-risk groups to these agents. Notably, ABT.263, ABT.888, AG.014699, AMG.706, Axitib had higher susceptibility in the High risk group and higher susceptibility to A.443654, A.770041, AUY922, AKT.inhibitor.VII,AZD.0530 in the low risk group, all of which indicated that PRGs was associated with drug susceptibility (Figure 8).

Discussion

Pancreatic adenocarcinoma(PAAD) is a highly aggressive cancer with an increasing incidence rate around the world, which the 5-year overall survival rate(OSA) reached only 6% and has changed little over the past few years[1, 2]. Due to its specific pathological progression and silent early-stage appearance, most PAAD patients develop clinical jaundice during more advanced stages, thus less than 20% of patients have options for surgical resection[2]. Continuous improvements have been applied to PAAD diagnostic approaches, and chemotherapy failed to achieve a satisfactory clinical outcome because of tumor heterogeneity and drug resistance[3]. Therefore, there is an urgent need for new potential diagnostic methods and treatment targets to provide a more comprehensive PAAD evaluation and prognostic system beneficial for all patients.

In recent years, with the advancement in investigation of cell death in cancer development, pyroptosis, an inflammatory form of programmed cell death (PCD), has become a new hallmark of the molecular mechanism underlying tumor progression, indicating potential roles in tumor diagnostic markers and treatment targets in cancers[4]. Previous studies have demonstrated that pyroptosis played a critical role in several types of cancers, including clear cell renal cell carcinoma (ccRCC) [5], lung squamous cell carcinoma(LUSC) [6], triple-negative breast cancer (TNBC) [7], epithelial ovarian cancer (EOC) [8], colorectal cancer (CRC) [9] and others. While the significant impacts on PAAD through pyroptosis-related genes (PRGs) has not been fully elucidated, many other aspects may influence tumor occurrence and progression simultaneously like tumor microenvironment(TME) [10]. Here, we conducted a novel, more comprehensive, and capable PAAD predictive risk model through pyroptosis pathways and PRGs to explore how these genes influence tumor progression and drug susceptibility and to provide a helpful PAAD evaluation system.

In our study, we screened 48 PAAD-related somatic mutational PRGs among 350 PAAD samples. The results showed that almost all of the PRGs (46 species) appeared significant higher in transcription levels compared with normal tissues. Take the gene GSDMC as an example, which constitute an important part of the gasdermin(GSDM) family that were first identified on chromosome 11 in a mouse model [11], it has been reported to play a potential clinical application in tumor therapy through cleavage by caspase-8 [12]. Thus, these indicated a potential role for PRGs in the development of PAAD.

To further explore specific expression characteristics of PAAD-related PRGs, principal component analysis (PCA) and subsequent K-M curve showed the expression levels of most PRGs and relapse-free survival (PFS) in subgroup B are much higher than counterparts of subgroup A and C, primarily indicating the predictive value of the expression levels of PRG. Then, by analyzing immunocyte subsets in 3 subgroups, an higher tendency in B-PRG cluster was shown accompanying an enrichment of cancer-related pathways, like cytokine receptors interaction and cell adhesion, indicating that pyroptosis may become one of the targets by TME variation to treat PAAD patients. A study by JianBin Wu et al reported an remarkably enriched in B cells, CD4 + T cells, CD8 + T cells, eosinophils, and T cell activation pathway of 33 PRGs in breast cancer patients [13], which was similar to our study in some aspects. Another previous investigation published by Guilong Tanzhu et al reported that a changing situation of immune infiltration in different subgroups has distinct correlations with risk score [14], no matter positive or negative correlation, and this situation was also remarkable in our study.

Based on the above characteristic, we classified the B-PRG cluster as the immune inflammation subgroup by immune cells infiltration and cellular pathway activation, revealing a potential role of PRGs expression in TME and PAAD progression, also bringing a molecular diagnosis target for clinical treatment.

Apart from the molecular level, we also investigate on a macroscopic perspective by developing a nomogram to predict survival. Our results showed that the PFS of 1,2 and 3 years had higher accuracy, and TP53 was the second most frequently mutated gene after KARS in high-risk and low-risk groups classified by PRG-score, which were previously mentioned [15, 16]. Besides the PRG-score utilized in our study, other similar assessment systems have been applied in the prognostic evaluation for PAAD patients. Ting Yu er al. Have developed a pyroptosis-ferroptosis(PF) score to analyze associated active immune phenotype, decreased genomic alterations, and predicting overall survival, revealing that the PAAD patients with low P-F score might be more sensitive to paclitaxel and 5-flfluorouracil [17]. Shanghai Bai, et al. have conducted a novel PR risk signature, an independent prognostic factor distinguishing different clinical subgroups, improving the traditional predictive models based on TNM-staging, and indicating that the overexpression of toll-like receptor 3 (TLR3) could promote the proliferation, migration, and invasion of PAAD cells [18]. These studies revealed potential targets underlying pyroptosis with PAAD for better clinical outcomes.

Finally, to provide better clinical treatment targets, we selected several chemotherapeutic agents currently used and found several agents had higher susceptibility in the higher risk group (ABT.263, ABT.888, AMG.706), which could also be seen in apoptosis pathways of other types of cancers, like oral cancer [19], glioma [20], low-grade neuroendocrine tumors [21]. On the contrary, some agents might have higher susceptibility in the lower risk group(A.443654, AUY922), which occurred in pathology of Parkinson's disease [22] and retinal toxicity [23]. These agents could further support PAAD treatment and reveal an interaction between pyroptosis and apoptosis, also elucidating innovative treatment regimen for cancers.

Although this is a relatively comprehensive and capable risk model for PAAD diagnostic and prognostic evaluation, there are limitations of our study. Firstly, our study is based on bioinformatics analysis, and

the results warranted corresponding animal or cell experiments to ultimately verify. Secondly, our data were obtained from several public database, and underlying age or sample bias may influence our results. Of course, pyroptosis is a relatively new aspect. It has not been fully elucidated, and more investigation about the interactions between pyroptosis and cancer are indicated to further the understanding of specific mechanism in PAAD.

In conclusion, as a newly founded programmed cell death, pyroptosis and PRGs play a pivotal role in the tumor microenvironment and tumor progression. Thus, we conducted a risk score model through bioinformatics technology by analyzing gene expression, immune cells infiltration, molecular subtypes, clinical stages, survival rate, gene mutation, and drug susceptibility to provide an overall evaluation system beneficial for further PAAD clinical diagnosis and prognosis, also bring new treatment targets and methods for PAAD patients.

References

1. Bai, Z., F. Xu, X. Feng, Y. Wu, J. Lv, Y. Shi and H. Pei (2022). "Pyroptosis regulators exert crucial functions in prognosis, progression and immune microenvironment of pancreatic adenocarcinoma: a bioinformatic and in vitro research." Bioengineered **13**(1): 1717–1735.
2. Bergsbaken, T., S. L. Fink and B. T. Cookson (2009). "Pyroptosis: host cell death and inflammation." Nat Rev Microbiol **7**(2): 99–109.
3. Bregetzer, J. (1989). "[Tele ... Life]." Rev Infirm **39**(19): 49–50.
4. Conesa, A., P. Madrigal, S. Tarazona, D. Gomez-Cabrero, A. Cervera, A. McPherson, M. W. Szcześniak, D. J. Gaffney, L. L. Elo, X. Zhang and A. Mortazavi (2016). "A survey of best practices for RNA-seq data analysis." Genome Biol **17**: 13.
5. Cookson, B. T. and M. A. Brennan (2001). "Pro-inflammatory programmed cell death." Trends Microbiol **9**(3): 113–114.
6. den Butter, G., J. H. van Bockel and J. C. Aarts (1988). "Arterial fibrodysplasia: rapid progression complicated by rupture of a visceral aneurysm into the gastrointestinal tract." J Vasc Surg **7**(3): 449–453.
7. Ding, J., K. Wang, W. Liu, Y. She, Q. Sun, J. Shi, H. Sun, D. C. Wang and F. Shao (2016). "Pore-forming activity and structural autoinhibition of the gasdermin family." Nature **535**(7610): 111–116.
8. Huang, X., G. Zhang, T. Tang and T. Liang (2021). "Identification of tumor antigens and immune subtypes of pancreatic adenocarcinoma for mRNA vaccine development." Mol Cancer **20**(1): 44.
9. Iacobuzio-Donahue, C. A., B. Fu, S. Yachida, M. Luo, H. Abe, C. M. Henderson, F. Vilardell, Z. Wang, J. W. Keller, P. Banerjee, J. M. Herman, J. L. Cameron, C. J. Yeo, M. K. Halushka, J. R. Eshleman, M. Raben, A. P. Klein, R. H. Hruban, M. Hidalgo and D. Laheru (2009). "DPC4 gene status of the primary carcinoma correlates with patterns of failure in patients with pancreatic cancer." J Clin Oncol **27**(11): 1806–1813.

10. Iasonos, A., D. Schrag, G. V. Raj and K. S. Panageas (2008). "How to build and interpret a nomogram for cancer prognosis." J Clin Oncol **26**(8): 1364–1370.
11. Ji, T., K. Ma, L. Chen and T. Cao (2021). "PADI1 contributes to EMT in PAAD by activating the ERK1/2-p38 signaling pathway." J Gastrointest Oncol **12**(3): 1180–1190.
12. Konstantinidis, I. T., A. L. Warshaw, J. N. Allen, L. S. Blaszkowsky, C. F. Castillo, V. Deshpande, T. S. Hong, E. L. Kwak, G. Y. Lauwers, D. P. Ryan, J. A. Wargo, K. D. Lillemoe and C. R. Ferrone (2013). "Pancreatic ductal adenocarcinoma: is there a survival difference for R1 resections versus locally advanced unresectable tumors? What is a "true" R0 resection?" Ann Surg **257**(4): 731–736.
13. Newman, A. M., C. L. Liu, M. R. Green, A. J. Gentles, W. Feng, Y. Xu, C. D. Hoang, M. Diehn and A. A. Alizadeh (2015). "Robust enumeration of cell subsets from tissue expression profiles." Nat Methods **12**(5): 453–457.
14. Nielsen, S. R., V. Quaranta, A. Linford, P. Emeagi, C. Rainer, A. Santos, L. Ireland, T. Sakai, K. Sakai, Y. S. Kim, D. Engle, F. Campbell, D. Palmer, J. H. Ko, D. A. Tuveson, E. Hirsch, A. Mielgo and M. C. Schmid (2016). "Macrophage-secreted granulin supports pancreatic cancer metastasis by inducing liver fibrosis." Nat Cell Biol **18**(5): 549–560.
15. Pipas, J. M., B. I. Zaki, M. M. McGowan, M. J. Tsapakos, G. H. Ripple, A. A. Suriawinata, G. J. Tsongalis, T. A. Colacchio, S. R. Gordon, J. E. Sutton, A. Srivastava, K. D. Smith, T. B. Gardner, M. Korc, T. H. Davis, M. Preis, S. M. Tarczewski, T. A. MacKenzie and R. J. Barth, Jr. (2012). "Neoadjuvant cetuximab, twice-weekly gemcitabine, and intensity-modulated radiotherapy (IMRT) in patients with pancreatic adenocarcinoma." Ann Oncol **23**(11): 2820–2827.
16. Rahib, L., B. D. Smith, R. Aizenberg, A. B. Rosenzweig, J. M. Fleshman and L. M. Matrisian (2014). "Projecting cancer incidence and deaths to 2030: the unexpected burden of thyroid, liver, and pancreas cancers in the United States." Cancer Res **74**(11): 2913–2921.
17. Rhim, A. D., E. T. Mirek, N. M. Aiello, A. Maitra, J. M. Bailey, F. McAllister, M. Reichert, G. L. Beatty, A. K. Rustgi, R. H. Vonderheide, S. D. Leach and B. Z. Stanger (2012). "EMT and dissemination precede pancreatic tumor formation." Cell **148**(1–2): 349–361.
18. Rooney, M. S., S. A. Shukla, C. J. Wu, G. Getz and N. Hacohen (2015). "Molecular and genetic properties of tumors associated with local immune cytolytic activity." Cell **160**(1–2): 48–61.
19. Shi, J., Y. Zhao, K. Wang, X. Shi, Y. Wang, H. Huang, Y. Zhuang, T. Cai, F. Wang and F. Shao (2015). "Cleavage of GSDMD by inflammatory caspases determines pyroptotic cell death." Nature **526**(7575): 660–665.
20. Wang, J., H. Zhang, P. Shao, X. Zhang and B. Zhou (2022). "Bioinformatic Analysis of Prognostic Value of Pyroptosis-Related Genes and Its Effect on Immune Cell Infiltration in Pancreatic Adenocarcinoma." Int J Gen Med **15**: 2311–2319.
21. Yang, H. C., S. L. Daniel, T. D. Hsu and H. L. Drake (1989). "Nickel transport by the thermophilic acetogen Acetogenium kivui." Appl Environ Microbiol **55**(5): 1078–1081.
22. Ye, Y., Q. Dai and H. Qi (2021). "A novel defined pyroptosis-related gene signature for predicting the prognosis of ovarian cancer." Cell Death Discov **7**(1): 71.

Figures

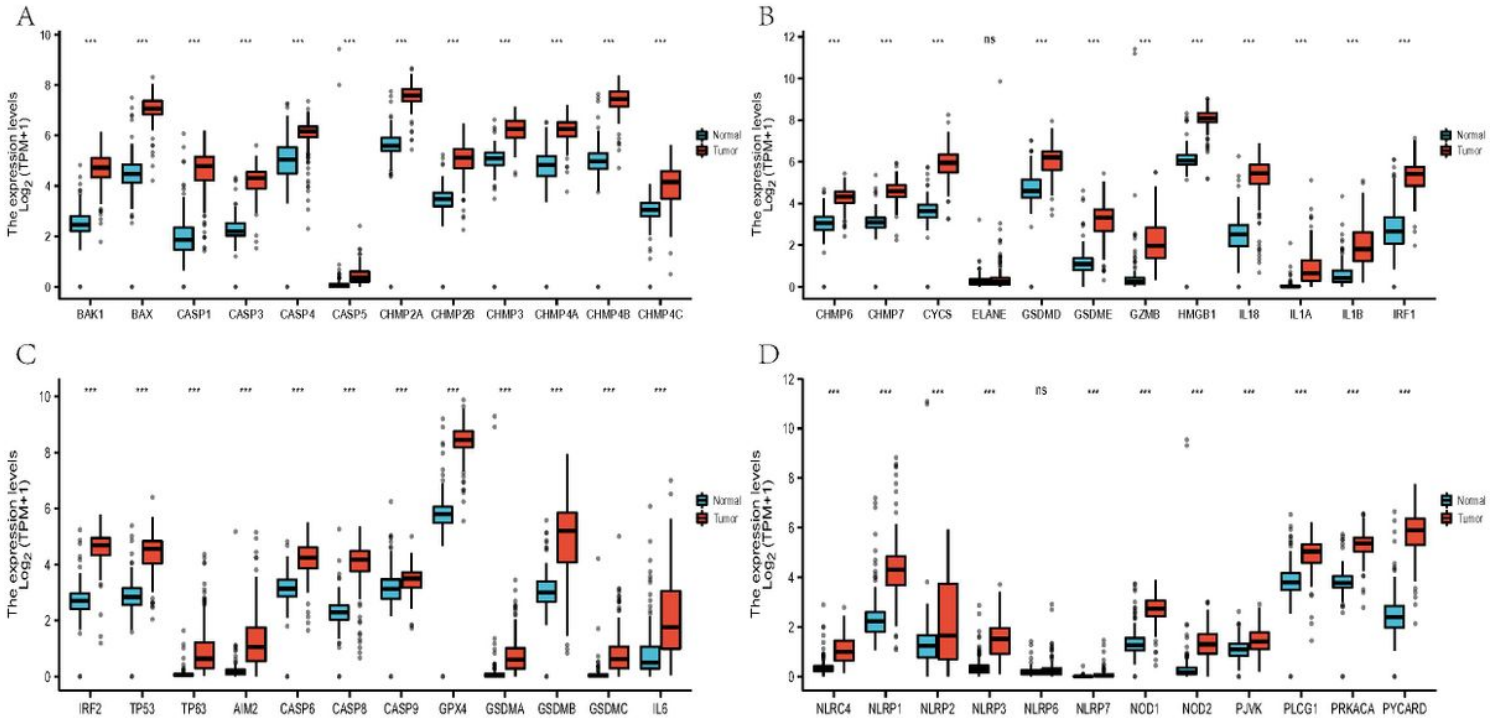

Figure 1

Differential expression of PRGs in tumor and normal tissues in PAAD. (**A-D**) Expression differences of 48 PRGs in 350 samples of pancreatic cancer.

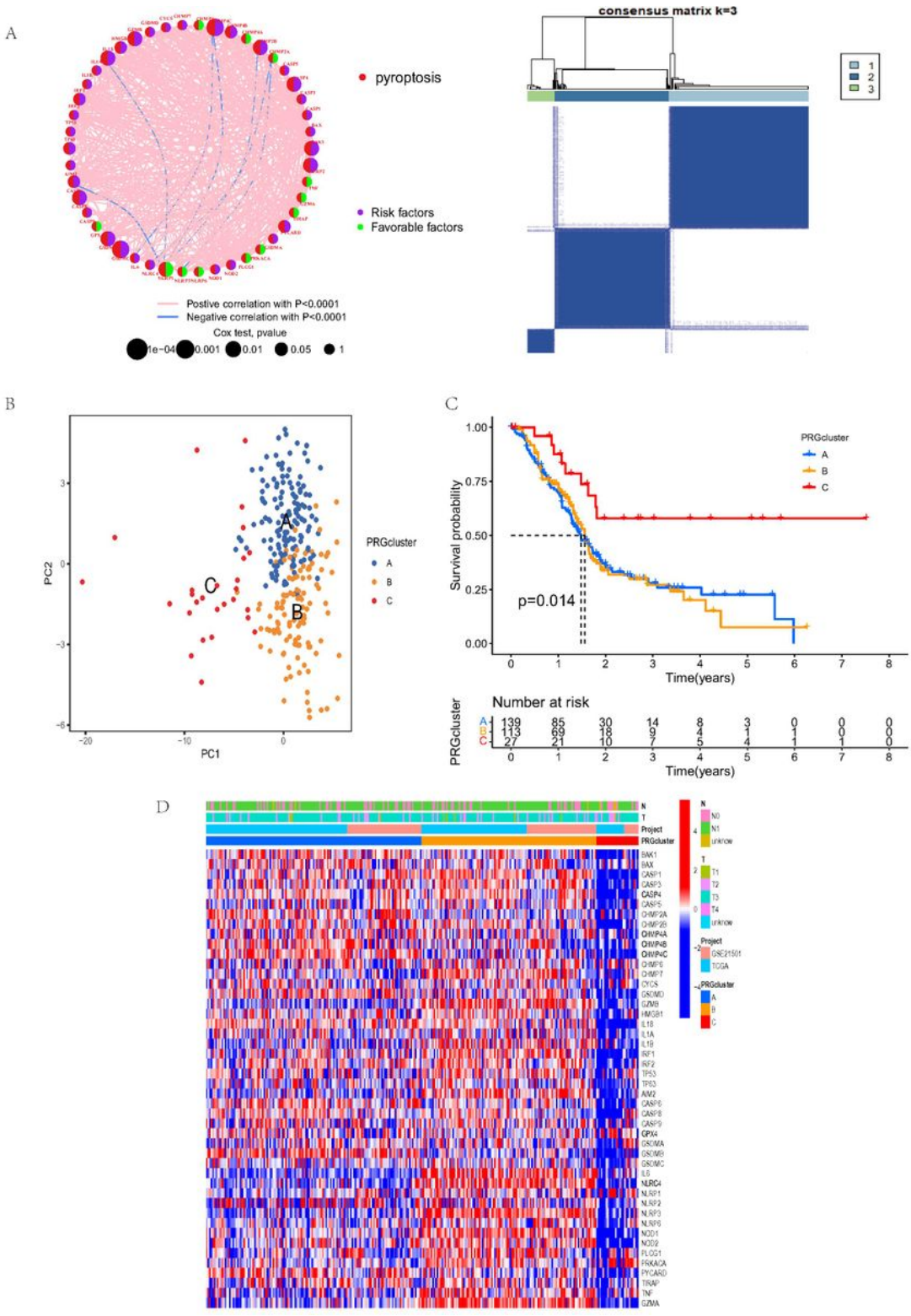

Figure 2

Subtypes of PRG and clinical pathology and biological characteristics of three different subtype samples by consistent clustering.

(A) Interactions between PRGs in PAAD. The lines connecting the PRGs represent their interactions, and Consensus matrix heatmap defining three clusters (k = 3) and their correlation area. (B) PCA suggested

there are obvious differences among the three subtypes. (C) Survival curves of three gene subtypes. (D) The correlations between PRG and different clinical variables, gene subtypes are shown by heat map.

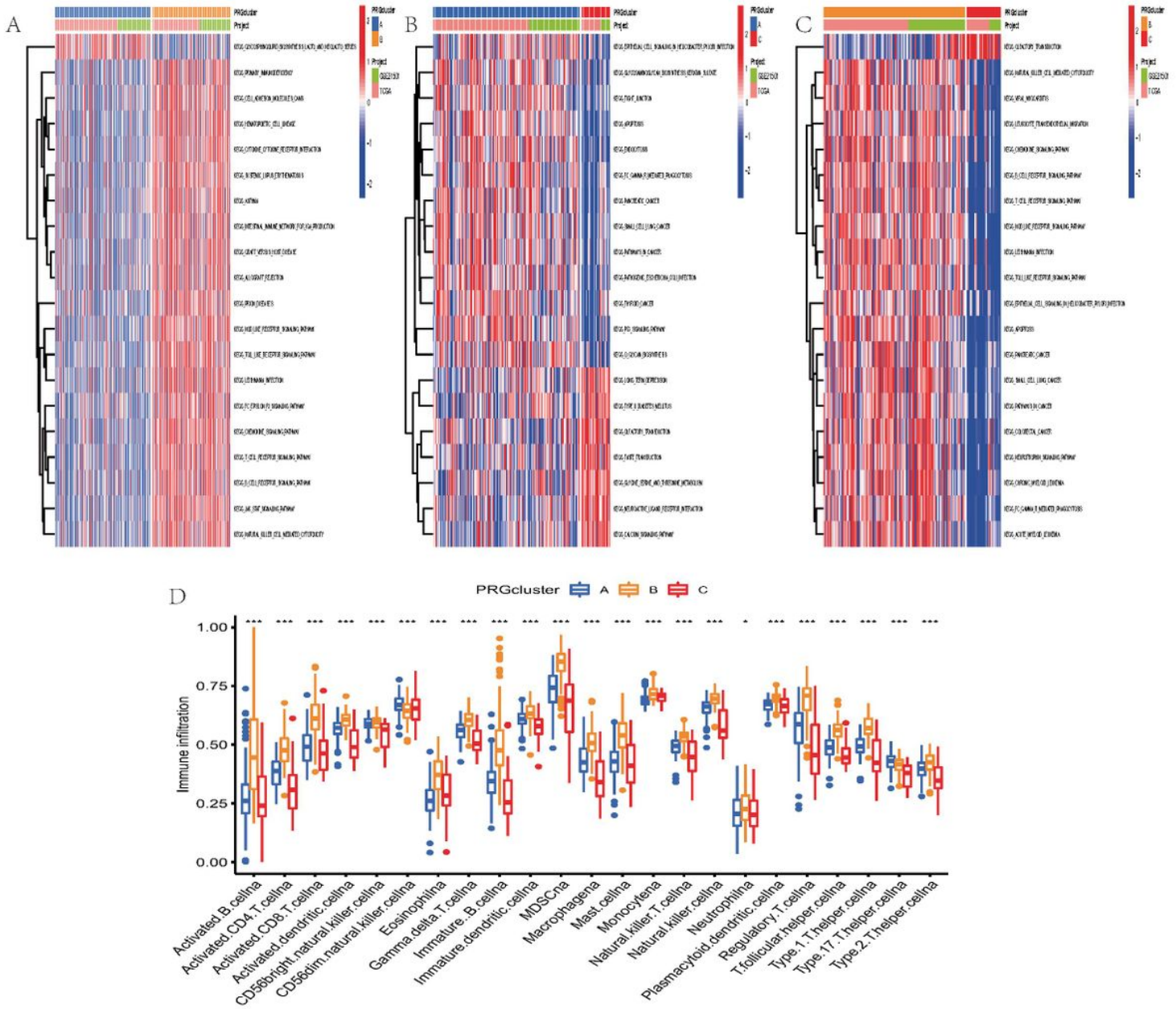

Figure 3

Relationship between different PGR subtypes and tumor immune microenvironment. (A-C) The heat map showed associations between three different genetic subtypes and the KEGG pathway. (D) Abundance of 22 infiltrating immune cell types in the three subtypes.

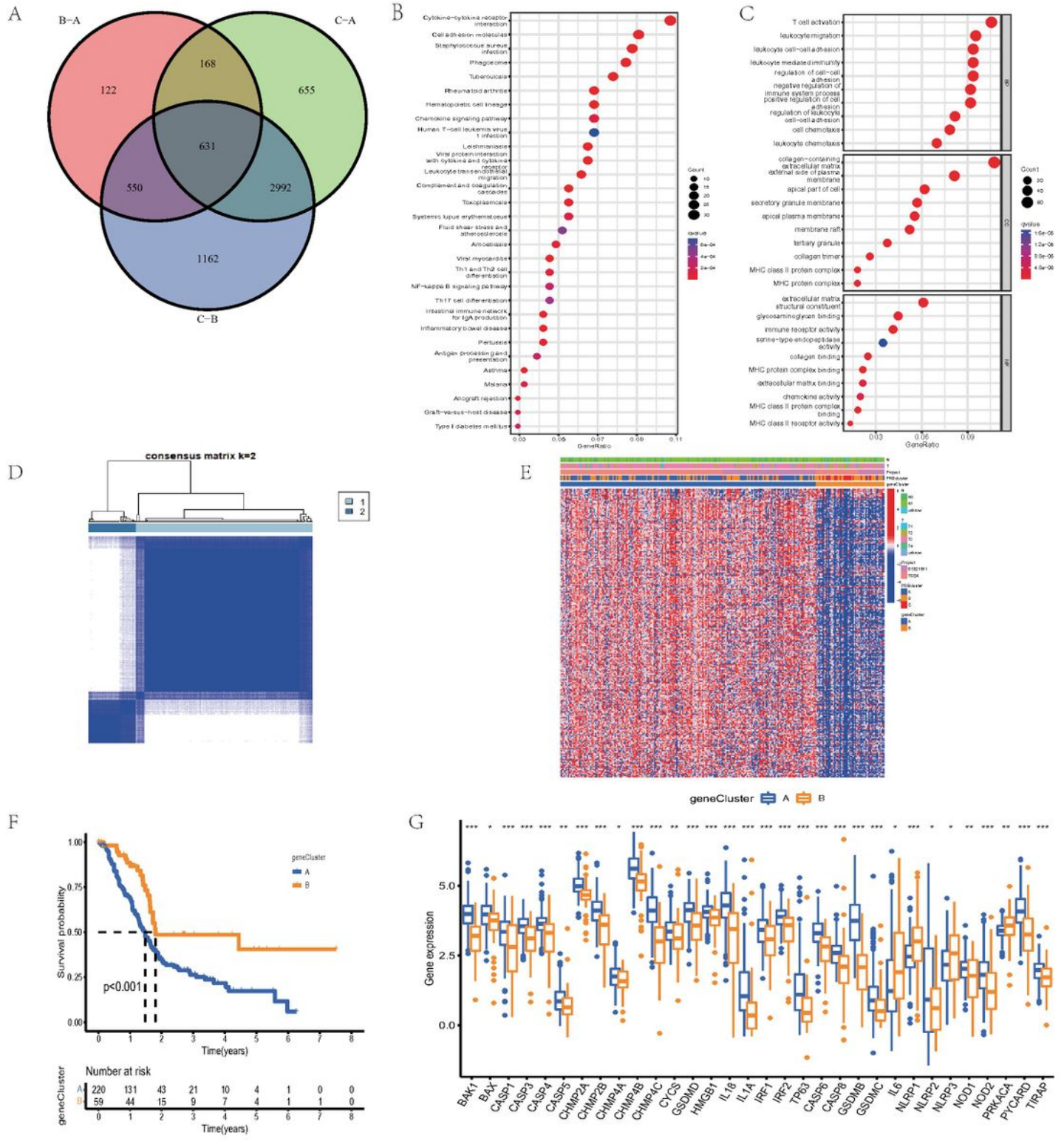

Figure 4

Identification of gene subtypes based on DEGs. (A) Common differential genes in three gene subtypes. (B-C) GO and KEGG enrichment analyses of DEGs. (D) Consensus matrix heatmap defining two clusters (k = 2). (E) Relationships between clinicopathologic features and the two gene subtypes. (F) Kaplan–Meier curves of the two gene subtypes (log-rank tests, p < .001). (G) Expression differences of 48 PRG between two gene subtypes.

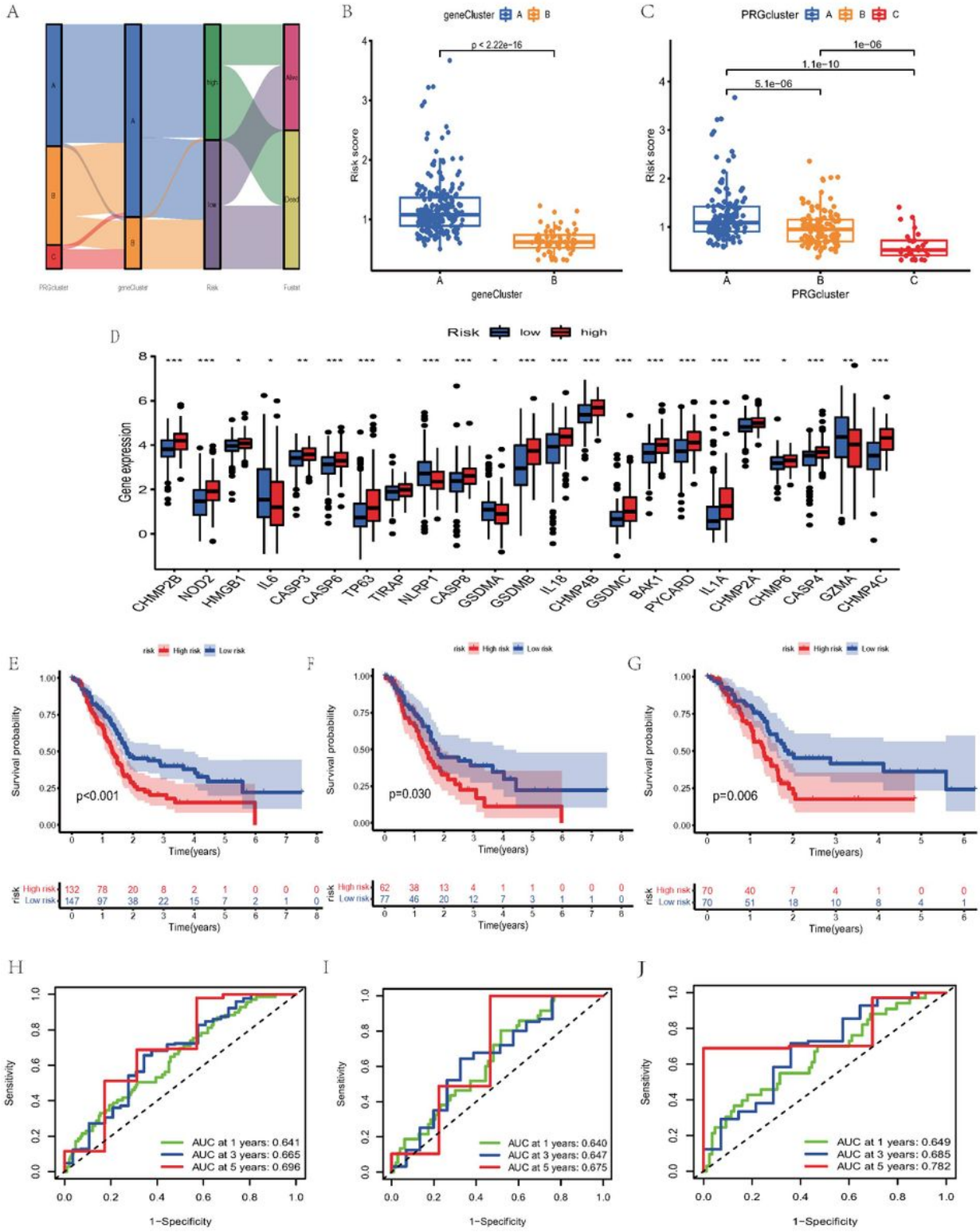

Figure 5

Construction of the PRG_score in the training set. (A) Alluvial plot of subtype distribution in groups with different PRG _ scores and survival results. (B) Differences in risk score between gene subtypes. (C) Differences in risk score between pyroptosis subtypes. (D) Expression of PRGs in the high and low-risk groups. (E-G) Kaplan–Meier analysis of the different prognosis types between the two groups. (H-J) ROC curves to predict the sensitivity and specificity of 1-, 3- and 5-year survival according to the risk score.

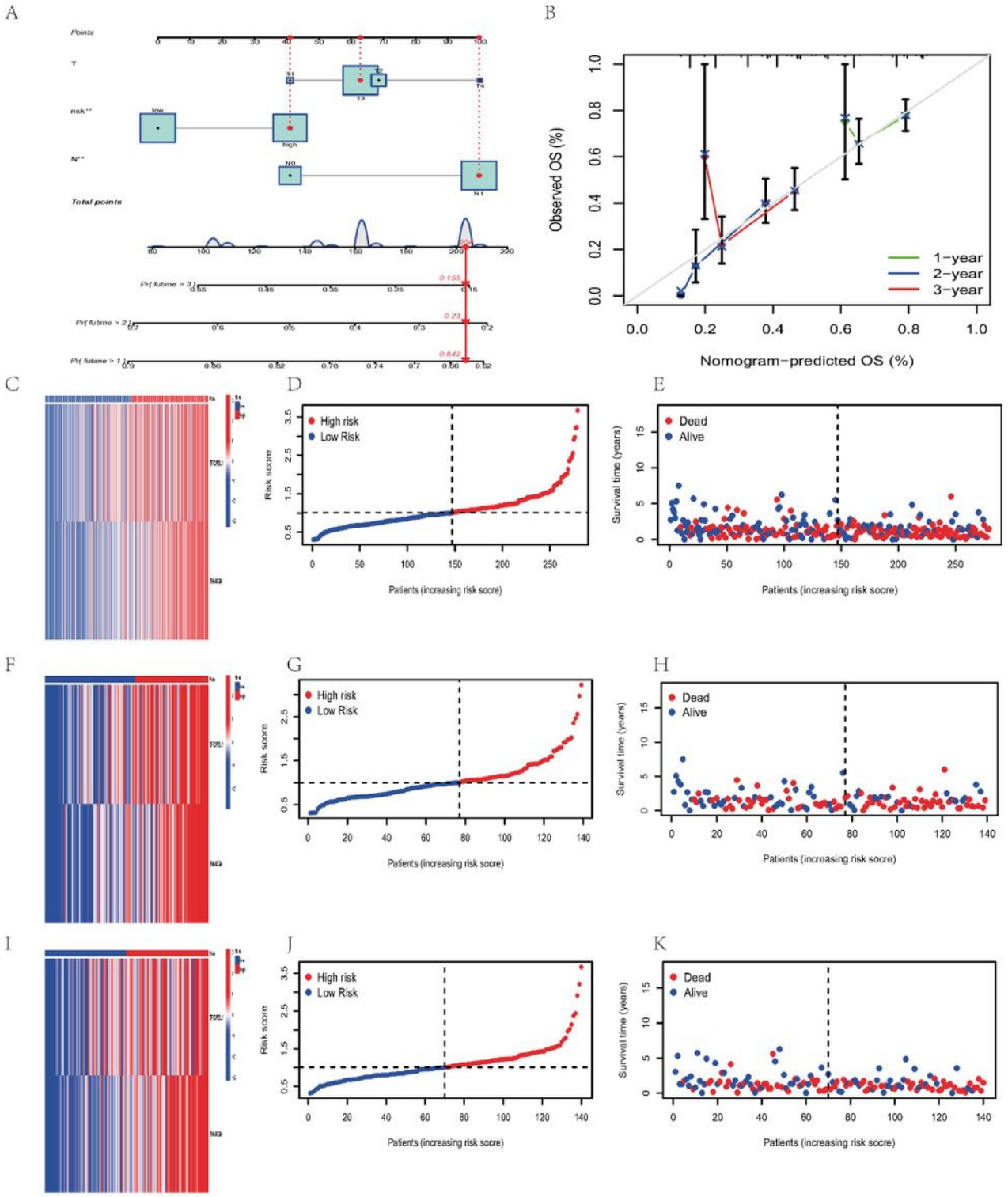

Figure 6

Construction and validation of a nomogram. (A) Nomogram for predicting the 1-, 2- and 3-year of PAAD patients in the training set. (B) Calibration diagram to illustrate the accuracy of the Nomogram model. (C-K) Ranked dot and scatter plots showing the risk score distribution and patient survival status.

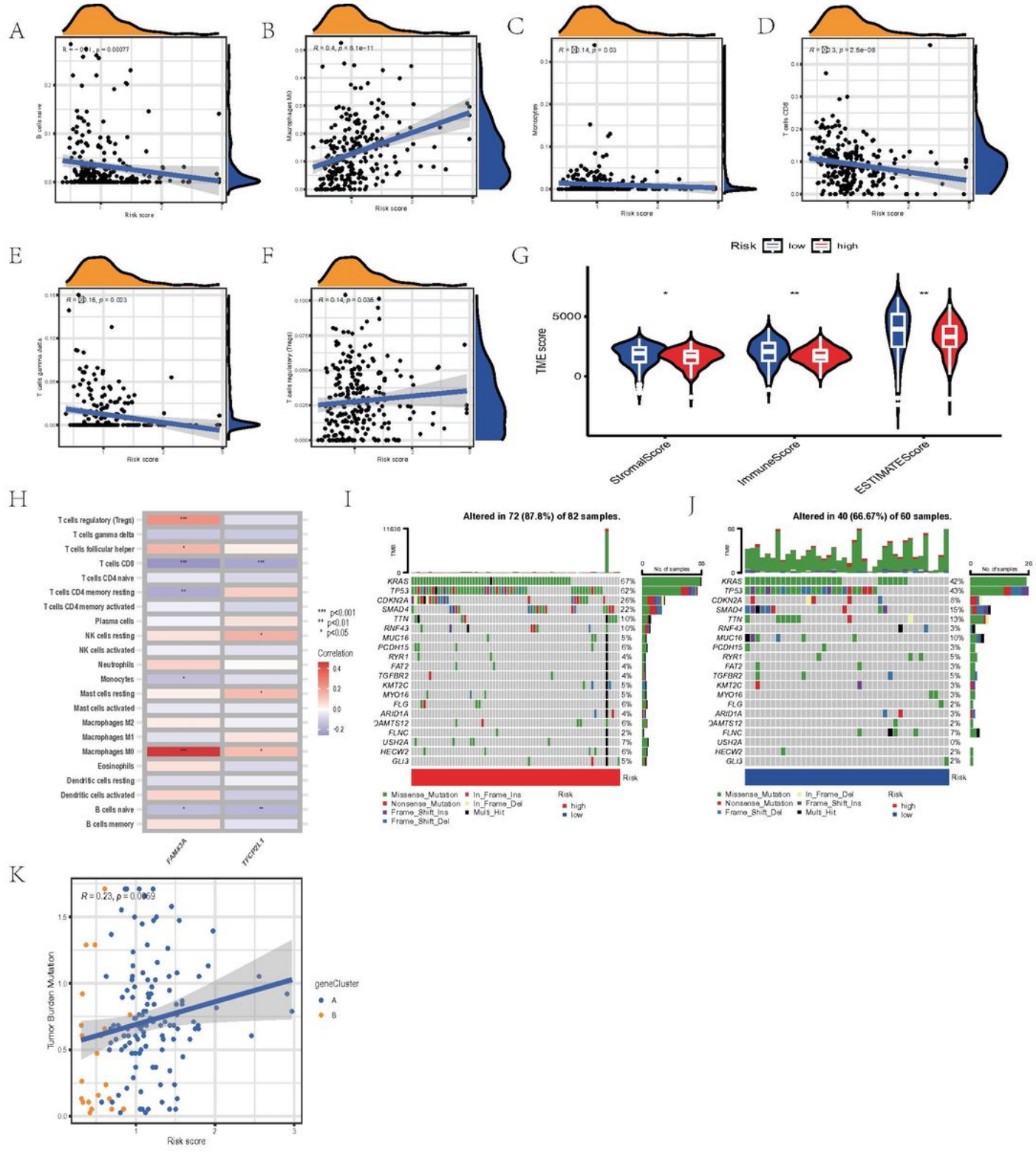

Figure 7

Assessment of TME and checkpoints between groups. (A-F) Correlations between PRG_score and immune cell types. (G) Correlations between PRG_score and both immune and stromal scores. (H) Correlations between the abundance of immune cells and seven genes in the proposed model. (I-J) A waterfall plot of somatic mutation characteristics was established with high and low risk scores. Each column represents one patient. The bar graph above shows TMB, and the number on the right shows the

mutation frequency of each gene. The bar chart on the right shows the scale for each variation type. (K) Spearman correlation analysis of the risk score and TMB.

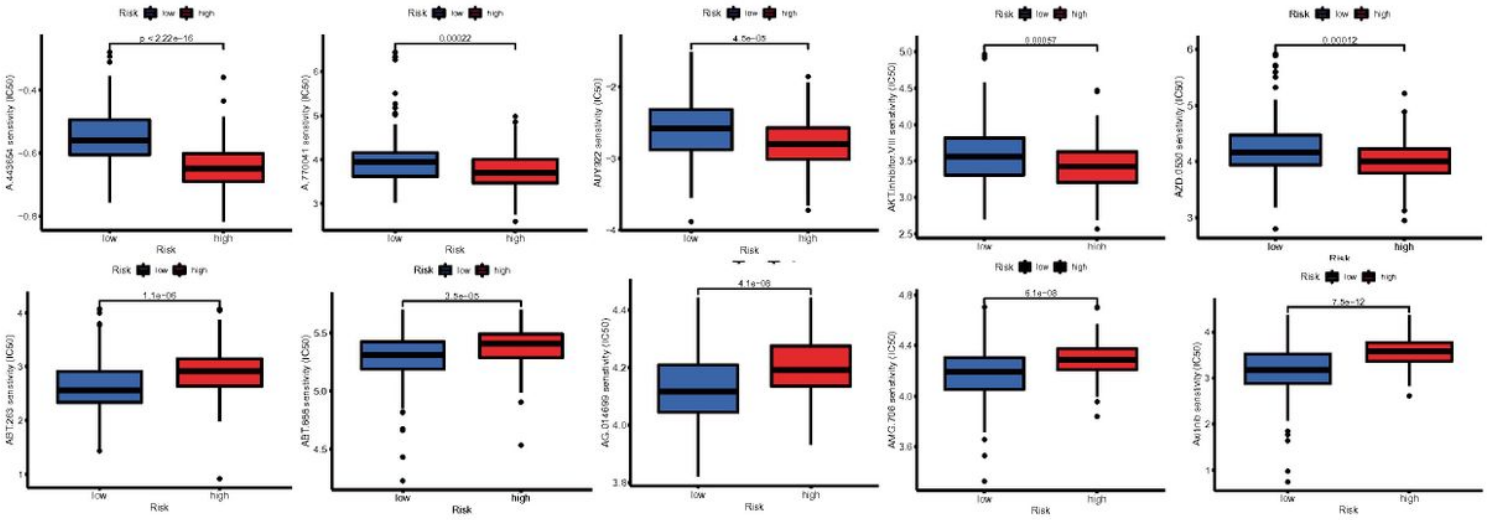

Figure 8

Differences in Sensitivity of Ten Anti-Cancer Drugs among Risk Groups